

# Stochastic quantum interferometry with Fock states

Francesco De Martini and Paolo Mataloni

*Dipartimento di Fisica and Istituto Nazionale per la Fisica della Materia, Università di Roma "La Sapienza,"  
Roma 00185, Italy*

Giovanni Di Giuseppe

*Dipartimento di Fisica and Istituto Nazionale per la Fisica della Materia, Università di Roma "La Sapienza,"  
Roma 00185, Italy, and Department of Electrical & Computer Engineering, Boston University, Boston,  
Massachusetts 02215-2421*

Fabrizio Altarelli

*Department of Physics, Harvard University, Cambridge, Massachusetts 02138*

Received March 14, 2001; revised manuscript received October 29, 2001

We report the experimental realization of first- and second-order optical stochastic interferometry with single-photon Fock states and with a couple of photons generated by spontaneous parametric downconversion. The behavior of the constitutive element of the stochastic interferometer, the stochastic beam splitter, is theoretically described, both for first- and second-order interferometry. The theory predicts a reduction of the visibility from 1 to  $\pi/4$  and to 1/2, respectively, for the two cases. These results are a direct consequence of the presence of Bose-Einstein correlations within the electromagnetic field. The visibility reduction obtained in the two experiments and their comparison with theoretical predictions are discussed in detail. © 2002 Optical Society of America

OCIS codes: 270.0270, 270.5290, 030.5260.

## 1. INTRODUCTION

Interferometry of quantum particles is rooted at the core of modern physics, as it provides a unique tool of investigation and a direct demonstration of fundamental natural properties such as complementarity, nonlocality, and quantum nonseparability.<sup>1-4</sup> The interferometer has generally been conceived so far as a stationary device, i.e., a measurement apparatus in which the transfer function  $w_i$  of the particle-scattering or beam-splitting elements are independent of time ( $t$ ). Only recently has the relevance of the  $t$ -dependent nonstationary, or stochastic, beam splitter (Sto-BS) been emphasized in connection with statistical properties of quantum particles. Examples are provided by a neutron interferometer having one arm regularly interrupted by a chopper,<sup>5,6</sup> by the intensity second-order optical correlator,<sup>7,8</sup> and by the first-order optical field stochastic interferometer<sup>9</sup> realized some years ago by our laboratory.<sup>10,11</sup> In the present study we first analyze the properties of the first-order stochastic interferometer (Sto-IF), and this is compared with the behavior of the usual stationary interferometer. As a paradigmatic example, Fig. 1 shows a Mach-Zehnder configuration in which the input two-way coherent scattering device is indeed provided by a stochastic beam splitter (Sto-BS) in which the probabilities of photon scattering over the output channels,  $W_i(t) \equiv |w_i(t)|^2$ , for  $i = 1, 2$  and  $\sum_i W_i(t) = 1$ , are made to vary in time within their existence range (0-1) by means of an external non-

stationary driving signal applied to an active electro-optical device. In other words, and more generally, we deal with the quite unusual case in which the amplitudes of the interfering particles' Feynman paths undergo an externally driven time perturbation: a peculiar quantum dynamical condition that, we believe, has never been investigated before. In particular, the driving parameters of the Sto-BS could vary on a time scale comparable to the transit time of the scattered particle through the interferometer. As previously remarked, this peculiar dynamical condition may open interesting perspectives in the context of the welcher-weg paradigm and in connection with delayed-choice-type experiments possibly involving more complicated systems, e.g., atom states in a micromaser.<sup>12,13</sup> As said, several experiments have already been devoted to the peculiar first-order Sto-IF condition in the optical range by adopting "stochastic" electro-optical (EO) devices.<sup>7,10,11</sup> The results obtained in these works were of course found to be a direct consequence of the basic linearity of quantum mechanics. However, all previous experiments were performed with "classical light," precisely a super-Poissonian Planckian light obtained by inducing stochastic phase disturbances on a single-mode laser beam. In view of the general arguments given above, it appears relevant to investigate the Sto-IF properties under the more significant excitation of "quantum," sub-Poissonian light, e.g., associated with an input Fock state generated by the modern technique of

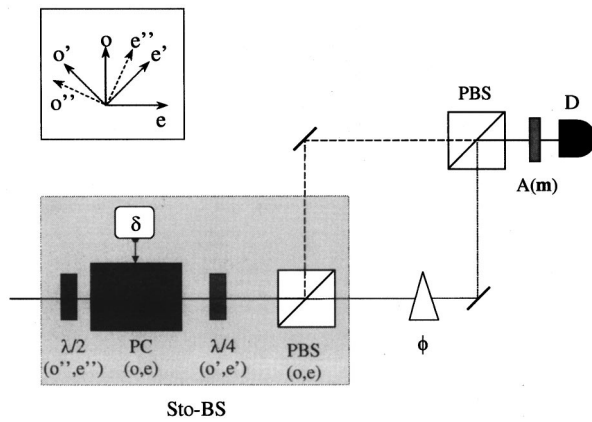


Fig. 1. First-order stochastic interferometer (Sto-If).

spontaneous parametric downconversion (SPDC) in a second-order nonlinear (NL) crystal.<sup>14</sup> In addition, in the present study we extend our investigation to the second-order stochastic quantum interferometer under excitation of a two-photon Fock state, again generated by SPDC. This study, never undertaken previously either theoretically or experimentally to our knowledge, extends into the stochastic domain the well known condition of two-photon excitation of a beam splitter, a condition of common interest in the modern field of quantum information.<sup>15–17</sup> Precisely in this domain, the new Sto-IF is expected to provide, for instance, a new variety of linear devices exhibiting new types of Hadamard unitary transformations.<sup>18</sup>

The paper is organized as follows. In Section 2 the general scattering theory of the optical lossless Sto-BS is presented. There it is shown that if the device is excited by an input single-mode Fock state, the particle partition statistics changes from the “classical,” Maxwell–Boltzmann to Bose–Einstein (BE) by increasing the spread of the distribution of the stochasticity parameter  $\sigma$ . A brief analysis of the BE condition given at the end of Section 2 emphasizes the peculiar general features of the stochastic scattering of particles over many output channels, of which the Sto-BS is but a significant example. Subsection 3.A reports the general theory of the first-order Sto-If with explicit calculations of the expected interference visibility, and Subsection 3.B accounts for the corresponding experimental demonstration. At last, the two subsections of Section 4 give a parallel, extended account of the second-order interferometry, both theory and experiment.

## 2. STOCHASTIC BEAM SPLITTER

The optical Sto-BS is a lossless device realized by means of a sequence of optical elements that introduce time-dependent changes on one (or several) degree of freedom of the state of the photon. In our case, the photon’s linear polarization ( $\pi$ ) is assumed to be a time-dependent variable, and the final beam-splitting process takes place in a (stationary) polarizing beam splitter, indicated by PBS in Fig. 1.

Assume that a single photon in a Fock state, generated by SPDC in a type II nonlinear crystal,<sup>19–21</sup> with linear

polarization ( $\pi$ ) oriented along the  $o$  axis, impinges on one port of a Sto-BS (Fig. 1). Consider the overall transmittivity ( $T \equiv |t|^2$ ) and the reflectivity ( $R \equiv |r|^2$ ) of the device. In virtue of the unitary property  $T + R = 1$ ,  $T$  and  $R$  can be also defined as

$$T = \frac{1+x}{2}, \quad R = \frac{1-x}{2},$$

where  $x$  is a stochastic parameter lying in the range  $[-1, 1]$ , with distribution  $p(x)$ . The general case of a Sto-BS driven by an arbitrary noise distribution  $p(x)$  has been investigated in Ref. 10. In the present paper we investigate the relevant case of a Gaussian distribution, with zero average value of the stochastic parameter,  $\bar{x} = 0$ , and related variance  $\sigma^2$ :

$$p(x|\sigma) \equiv \frac{1}{\sqrt{2\pi}\sigma \operatorname{erf}\left(\frac{1}{\sqrt{2}\sigma}\right)} \exp\left[-\left(\frac{x}{\sqrt{2}\sigma}\right)^2\right], \quad (1)$$

where the normalization condition  $\int_{-1}^1 p(x|\sigma) dx = 1$  holds. Two extreme relevant cases are considered:

$\sigma \rightarrow 0$ :  $p(x|\sigma)$  is equivalent to a Dirac  $\delta$  function. This corresponds to the case of an ordinary symmetric beam splitter, with  $R = T = 1/2$ .

$\sigma \rightarrow \infty$ :  $p(x|\sigma)$  is a constant,  $\lim_{\sigma \rightarrow \infty} p(x|\sigma) = 1/2$ . This corresponds to a uniform distribution of  $R(x) = |r|^2$  and  $T(x) = |t|^2$  in the range  $[0-1]$ .

We may analyze the physical conditions underlying this process by referring to the scheme described in Fig. 1. The input photon is transmitted through a sequence of three optical elements: a half-wave plate ( $\lambda/2$ ), an externally driven Pockels cell (PC), and a quarter-wave plate ( $\lambda/4$ ). The optical axes of the three elements are oriented along the directions  $o''-e''$ ,  $o-e$ , and  $o'-e'$ , respectively (inset of Fig. 1). Finally, the output signal impinges on a polarizing beam splitter (PBS) where it is decomposed in two orthogonal  $\pi$  components, oriented along the axes  $o$  and  $e$ .

Consider the effect induced on the photon’s polarization state by the various elements of Sto-BS. By assuming the polarizations eigenstates  $o$  and  $e$  to be coincident with

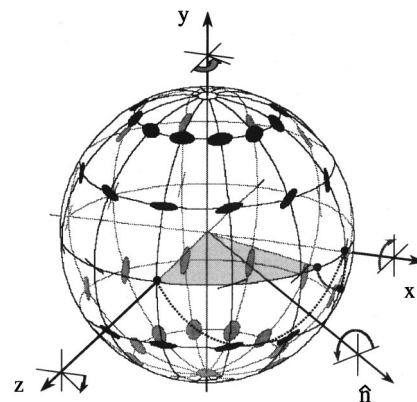


Fig. 2. Poincaré sphere representation of the rotation performed by the stochastic beam splitter on the input single-photon state.

eigenstates of  $\hat{\sigma}_z$  with eigenvalues  $+1$  and  $-1$ ,  $|o\rangle \equiv |+\rangle$  and  $|e\rangle \equiv |-\rangle$ , we refer to the Poincaré sphere shown in Fig. 2.<sup>22</sup>

The first half-wave plate ( $\lambda/2$ ) causes a rotation of  $\pi$  around its proper axes, the vector  $\mathbf{n}$ ; this action is defined by the operator

$$\hat{U}^{(1)} = \exp\left(-i\frac{\pi}{2}\mathbf{n} \cdot \hat{\boldsymbol{\sigma}}\right) = -i\mathbf{n} \cdot \hat{\boldsymbol{\sigma}}, \quad (2)$$

which, for  $\mathbf{n} = \{1/\sqrt{2}, 0, 1/\sqrt{2}\}$ , can be expressed as

$$\hat{U}^{(1)} = \frac{-i}{\sqrt{2}}(\hat{\sigma}_x + \hat{\sigma}_z). \quad (3)$$

The electro-optic Pockels cell (PC) contributes with a rotation  $\delta$  around  $\hat{\sigma}_z$ , which gives

$$\hat{U}^{(2)} = \exp\left(-i\frac{\delta}{2}\hat{\sigma}_z\right) = \cos\frac{\delta}{2}\hat{I} - i\sin\frac{\delta}{2}\hat{\sigma}_z. \quad (4)$$

The quarter-wave plate ( $\lambda/4$ ) is oriented to introduce a rotation of  $\pi/2$  around the  $x$  axes:

$$\hat{U}^{(3)} = \exp\left(i\frac{\pi}{2}\hat{\sigma}_x\right) = \frac{1}{\sqrt{2}}(\hat{I} + i\hat{\sigma}_x). \quad (5)$$

By combining Eqs. (3), (4), and (5), we have

$$\hat{U} = \hat{U}^{(3)} \cdot \hat{U}^{(2)} \cdot \hat{U}^{(1)} = \hat{R}_y\left(\delta + \frac{\pi}{2}\right) \cdot \hat{R}_z\left(\frac{\pi}{2}\right), \quad (6)$$

where

$$\hat{R}_j(\theta) = \exp\left(-i\frac{\theta}{2}\hat{\sigma}_j\right). \quad (7)$$

The overall expression (6) can be finally written in the matrix form:

$$\hat{U} = \begin{bmatrix} \cos\left(\frac{\delta}{2} + \frac{\pi}{4}\right)\exp\left(-i\frac{\pi}{4}\right) - \sin\left(\frac{\delta}{2} + \frac{\pi}{4}\right)\exp\left(+i\frac{\pi}{4}\right) \\ \sin\left(\frac{\delta}{2} + \frac{\pi}{4}\right)\exp\left(-i\frac{\pi}{4}\right) \cos\left(\frac{\delta}{2} + \frac{\pi}{4}\right)\exp\left(+i\frac{\pi}{4}\right) \end{bmatrix}. \quad (8)$$

The expressions of the transmission and reflection coefficients of the PBS are

$$t = \cos\left(\frac{\delta}{2} + \frac{\pi}{4}\right)\exp\left(-i\frac{\pi}{4}\right),$$

$$r = \sin\left(\frac{\delta}{2} + \frac{\pi}{4}\right)\exp\left(+i\frac{\pi}{4}\right).$$

This leads to the expressions of the transmissivity and reflectivity of the Sto-BS,

$$T = |t|^2 = \frac{1 + \sin\delta}{2}, \quad R = |r|^2 = \frac{1 - \sin\delta}{2}, \quad (9)$$

where the stochastic parameter is  $\sin\delta = x$ . The behavior of the Sto-BS is determined by the nonstationary character of the phase angle  $\delta$ , which is related to the external

electric signal applied to the PC. In the experiment reported here, the electric signal was a periodic function of time, and the stochasticity of  $x$ , with Gaussian distribution function  $p(x|\sigma)$ , arose from the random arrival time of the photon on the Sto-BS.

We may write, for example, the action of the operator  $\hat{U}$  on the  $o$  polarization of the input single-photon pure state,  $|\Psi\rangle_{\text{in}} = |o\rangle$ :

$$\begin{aligned} |\Psi\rangle_{\text{int}} &= \hat{U}|\Psi\rangle_{\text{in}} \\ &= \exp\left(-i\frac{\pi}{4}\right)\left[\cos\left(\frac{\delta}{2} + \frac{\pi}{4}\right)|o\rangle + \sin\left(\frac{\delta}{2} + \frac{\pi}{4}\right)|e\rangle\right], \end{aligned} \quad (10)$$

where  $|\Psi\rangle_{\text{int}}$  is the intermediate polarization state just after the Sto-BS.

### A. Bose–Einstein Correlations by Stochastic Two-Way Scattering

It can be enlightening to analyze in more detail the stochastic partition over the two ( $M = 2$ ) output modes  $i = 1, 2$  of the lossless Sto-BS of  $n$  particles associated with a Fock state  $|n\rangle$  and injected into one of the input modes of the device, the other input mode being in the vacuum state  $|0\rangle$ .<sup>7–11</sup> Consider the partition probability  $P_{nh}$  of the  $n$  input particles into  $h$  and  $(n - h)$  output particles. In the case of stationary BS splitting (i.e., by a Sta-BS) with elementary probabilities  $W_1$  and  $W_2 = 1 - W_1$ , this quantity is expressed by the well known Bernoulli distribution  $P_{nh} = W_1^{(n-h)}W_2^h C_h^n$ ,  $C_h^n \equiv [n!/h!(n-h)!]$  expressing “classical” absence of photon correlations in the BS process. When the splitting is carried out by the Sto-BS, the above expression is replaced more generally by

$$P_{nh} = 2^{-n} C_h^n \int_{-1}^{+1} [(1+x)^{(n-h)}(1-x)^h] p(x|\sigma) dx. \quad (11)$$

The Sta-BS condition is easily recovered by setting  $\sigma = 0$  in Eq. (1):  $p(x|\sigma) = \delta(x)$ . The opposite condition  $\sigma \rightarrow \infty$  implies the uniform distribution  $\lim_{\sigma \rightarrow \infty} p(x|\sigma) = 1/2$ , which in turn implies a driven, deterministic correlation of the state on the output particles. The corresponding value of the integral is found to be generally expressed in terms of gamma functions by the beta function<sup>23</sup>:  $B[(n-h+1), (h+1)] \equiv \Gamma(n-h+1)\Gamma(h+1)/\Gamma(n+2)$ . This leads in our case to the result  $P_{nh} = (n+1)^{-1}$  expressing the Bose–Einstein (BE) partition law of  $n$  particles over  $M = 2$  boxes, i.e., output modes. This result has been tested experimentally.<sup>7</sup> Interestingly enough, the realization of the general BE partition law  $(P_{nh})_{\text{BE}} = n!(M-1)!/(n+M-1)!$  of  $n$  photons over a very large number of output scattering channels  $M \gg 2$  has also been successfully tested in a set of experiments in which a single laser beam was stochastically (elastically) scattered by an ensemble of small polystyrene particles in Brownian motion at various temperatures  $\bar{T}$ . There the transition from BE to classical partition statistics was recovered by freezing of the motion of the scattering particles at low  $\bar{T}$ .

Equation (11) was first introduced by Laplace and investigated in detail by De Finetti in the context of exchangeable sequences in probability theory.<sup>24, 25, 26</sup> In this context it might be found at first sight surprising that the visibility  $V$  of the output patterns of the first- and second-order interferometers is lowered in the case of Sto-BS in respect to the maximum value obtained with a Sta-BS. We may easily clarify this point as follows. We have shown<sup>10,11</sup> that the attainment in the former case of a true photon Bose–Einstein condensation over the two interferometer modes implies a reduction,  $-\Delta H_{\text{loc}}$ , of the particle-localization information entropy (i.e., accounting for the particlelike photon's character) from the maximum value  $H_{\text{loc}} = \ln 2 = 0.693$  to the value  $H_{\text{loc}} = 0.50$ . This implies a corresponding increase by  $\Delta H_{\text{loc}}$  of the information entropy related to the complementary photon's wave-like property, and consequently it leads to a loss of fringe visibility. More physically, the deterministic routing effect induced by the Sto-BS on the input photon beam spoils the complete aleatory character of the coherent scattering property of the Sta-BS. The price paid for the in-principle information gained on the path taken by the particle emerging from the Sto-BS is precisely a loss of fringe visibility. Of course, this is a well known feature of all quantum phenomena ascribable to Bohr's complementarity. If we keep analyzing the interference phenomena reported here in the context of quantum information, we may note that the perturbation of the aleatory scattering character of the input BS of the interferometer, and then the  $-\Delta H_{\text{loc}}$  decrease of the information content of the system, may be viewed as a kind of decoherence on the state of the photon. In fact, in virtue of this decoherence process the pure qubit state implied by the normal (i.e., Sta-BS) two-way interferometer is transformed by the effect of the Sto-BS into a mixed state. The detected loss of fringe visibility may be indeed related formally to the complex parameter of this mixing process.

### 3. THEORY OF FIRST-ORDER STOCHASTIC INTERFEROMETRY

We refer to our model first-order stochastic interferometer, the Mach–Zehnder Sto-If shown in Fig. 1. The input beam is split by the Sto-BS in two different paths corresponding to the orthogonal  $\pi$  polarizations  $o$  and  $e$ , before being recombined at the output by a stationary polarizing beam splitter PBS. If  $\phi$  represents the phase difference between the two arms of the interferometer, the output state can be expressed as

$$\begin{aligned} |\Psi\rangle_{\text{out}} &= \hat{R}_z(\phi)|\Psi\rangle_{\text{int}} \\ &= \hat{R}_z(\phi)\hat{U}|\Psi\rangle_{\text{in}} = \hat{U}(R)|\Psi\rangle_{\text{in}}. \end{aligned} \quad (12)$$

In this expression,  $\phi = 4\pi\delta z/\lambda$ , where  $\delta z$  represents the length difference of the two arms.

We can also write

$$\hat{\rho}_{\text{out}}(\mathbf{p}) = \hat{U}(R)\hat{\rho}_{\text{in}}(\mathbf{n})\hat{U}^\dagger(R) = \frac{\hat{I} + \mathbf{p} \cdot \hat{\sigma}}{2}, \quad (13)$$

where  $\hat{\rho}_{\text{in}}(\mathbf{n})$  is defined as

$$\hat{\rho}_{\text{in}}(\mathbf{n}) = |o\rangle\langle o| = \frac{\hat{I} + \mathbf{n} \cdot \hat{\sigma}}{2}, \quad (14)$$

with  $\mathbf{n} = \{0, 0, 1\}$ . By means of the isomorphism between the two-dimensional polarization Hilbert space and the three-dimensional Poincaré sphere space,<sup>27, 28</sup> we obtain

$$\hat{U}(R)\mathbf{n} \cdot \hat{\sigma}\hat{U}^\dagger(R) = \mathbf{n} \cdot R\hat{\sigma} = R^T\mathbf{n} \cdot \hat{\sigma}. \quad (15)$$

In this way we obtain  $\mathbf{p} = R^T\mathbf{n}$ . The rotation matrix  $R$  associated with  $\hat{U}(R)$  is

$$\begin{aligned} R &= R_z\left(\frac{\pi}{2}\right)R_y\left(\delta + \frac{\pi}{2}\right)R_z(\phi) \\ &= \begin{bmatrix} -\sin\phi & \cos\phi & 0 \\ -\cos\phi\sin\delta & -\sin\phi\sin\delta & \cos\delta \\ \cos\phi\cos\delta & \sin\phi\cos\delta & \sin\delta \end{bmatrix}, \end{aligned} \quad (16)$$

where  $R_j(\theta)$  is the matrix for the  $\theta$  angle rotation around the  $j$  axes.

The last element of the interferometer shown in Fig. 1 consists of the polarization analyzer  $A(\mathbf{m})$ , inserted after the output BS and in front of the detector  $D$ .  $A(\mathbf{m})$  selects the polarization component along the direction  $\mathbf{m}$  and creates the conditions to observe the interference fringe pattern.

A convenient expression of the fringe visibility is obtained by evaluating the photon-detection probability:

$$\begin{aligned} P(\mathbf{m}, \pm) &= \text{Tr}\left[\frac{1 \pm \mathbf{m} \cdot \hat{\sigma}}{2}\hat{\rho}_{\text{out}}(\mathbf{p})\right] \\ &= \text{Tr}\left[\frac{1 \pm \hat{U}^\dagger(R)\mathbf{m} \cdot \hat{\sigma}\hat{U}(R)}{2}\hat{\rho}_{\text{in}}(\mathbf{n})\right]. \end{aligned} \quad (17)$$

Since a rotation  $R$  of the state is equivalent to a rotation by  $R^{-1}$  of the measurement apparatus, we get

$$\begin{aligned} P(\mathbf{m}, \pm) &= \frac{1}{2}[1 \pm \mathbf{m} \cdot R^T\mathbf{n}] = \frac{1}{2}[1 \pm \mathbf{m} \cdot \mathbf{p}] \\ &= \frac{1}{2}[1 \pm R\mathbf{m} \cdot \mathbf{n}]. \end{aligned} \quad (18)$$

For a  $45^\circ$  orientation of  $\mathbf{m}$  in respect to  $o$ ,  $\mathbf{m} = \{1, 0, 0\}$  ( $o'$  axis) is obtained:

$$P(\delta, \varphi) = \frac{1}{2}(1 \pm \cos\delta\cos\varphi). \quad (19)$$

The instantaneous value of the first-order fringe visibility, defined as  $V^{(1)} = I_{\text{max}} - I_{\text{min}}/I_{\text{max}} + I_{\text{min}}$ , becomes

$$V^{(1)}(\delta) = |\cos\delta|, \quad (20)$$

with  $-\pi/2 \leq \delta \leq \pi/2$ . The average value of the visibility with respect to  $x$ ,  $V^{(1)}(x) = (1 - x^2)^{1/2}$ , is given by the expression

$$\langle V^{(1)}(x) \rangle_x = \int_{-1}^{+1} p(x)V^{(1)}(x)dx. \quad (21)$$

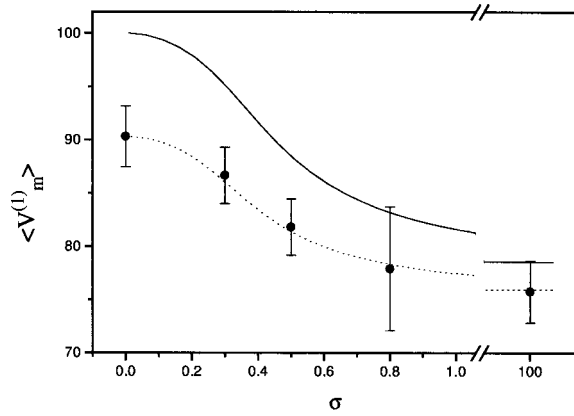


Fig. 3. First-order fringe visibility  $\langle V^{(1)} \rangle$ , Eq. (22), as a function of the stochastic parameter  $\sigma$ : the solid curve represents the theoretical prediction; the dotted curve corresponds to the best-fit analysis of the experimental data.

The evaluation of the integral may be given by use of the expression (1) for  $p(x)$ .

By adopting the integral representation of the hypergeometric function  ${}_1F_1(a, b; z)$  the expression of the first-order visibility is<sup>23</sup>

$$\langle V^{(1)} \rangle(\sigma) = \frac{\pi}{4} \frac{{}_1F_1\left[\frac{3}{2}, 2; \frac{1}{2\sigma^2}\right]}{{}_1F_1\left[1, \frac{3}{2}; \frac{1}{2\sigma^2}\right]}. \quad (22)$$

Exactly the same result is obtained by the explicit evaluation of the integrals within the following general expression for the first-order visibility evaluated<sup>10</sup> by a different theoretical approach:

$$\langle V^{(1)} \rangle(\sigma) = \frac{\pi}{2} \frac{\int_{-\infty}^{+\infty} P(\chi) \frac{J_1(2\pi\chi)}{\chi} d\chi}{\int_{-\infty}^{+\infty} P(\chi) \frac{\sin(2\pi\chi)}{\chi} d\chi}. \quad (23)$$

Here  $J_1(2\pi\chi)$  is a Bessel function and  $P(\chi) \equiv [\text{erf}(\sqrt{2}\sigma)^{-1}]^{-1} \exp[-(\sqrt{2}\pi\sigma\chi)^2]$  is the Fourier transform of the Gaussian  $p(x|\sigma)$ . The function  $\langle V^{(1)} \rangle(\sigma)$  is reported in Fig. 3 (solid curve) as a function of the noise parameter  $\sigma$  in the range 0–100. For  $\sigma \rightarrow \infty$ , i.e., for a fully white-noise spectrum, the asymptotic expansion  ${}_1F_1(a, b; z)$  leads to the limit value:  $\langle V^{(1)} \rangle(\infty) = \pi/4 \approx 0.785$ .<sup>7,10</sup> The other limit  $\sigma = 0$ , corresponding to the common stationary first-order interferometry, leads to the well known value  $\langle V^{(1)} \rangle(0) = 1$  independent of the average number of particles  $\langle n \rangle$  associated with the input state.<sup>10</sup>

#### A. Experiment

In view of the configuration of our experiment we first find it convenient to express the average first-order visibility as a function of  $\delta$ :

$$\langle V_m^{(1)} \rangle = \frac{1}{\Delta T} \int_{\Delta T} V^{(1)}(\delta) dt. \quad (24)$$

In the above expression,  $\Delta T$  represents the characteristic period of variation of  $\delta$ . We need to consider the simultaneous realization of the two conditions: (a)  $\Delta T \gg \Delta T'$ , where  $\Delta T'$  is the transit time of the photon through the Sto-BS, and (b)  $\Delta T \ll \Delta T''$ , where  $\Delta T''$  corresponds to the time necessary to collect the statistical ensemble of photocounts for each value of the phase shift  $\phi$ . Both conditions are easily satisfied in the experiment because  $\Delta T'$  is in the picosecond time domain, and  $\Delta T''$  can be of the order of a second. Since  $x = \sin \delta$ , we make use of the following condition:

$$\frac{1}{\Delta T} dt = p(x|\sigma) dx. \quad (25)$$

As a consequence,

$$\frac{dt}{dx} = \Delta T p(x|\sigma) = \frac{\Delta T}{\sqrt{2\pi\sigma} \text{erf}\left(\frac{1}{\sqrt{2}\sigma}\right)} \exp\left[-\left(\frac{\sin \delta}{\sqrt{2}\sigma}\right)^2\right]. \quad (26)$$

We may express the first-order visibility in the form

$$\langle V_m^{(1)} \rangle = \frac{1}{\Delta T} \int_{-\pi/2}^{\pi/2} V(\delta) \frac{dt}{dx} \frac{dx}{d\delta} d\delta, \quad (27)$$

where  $dx/d\delta = \cos \delta$ . It is obtained

$$\langle V_m^{(1)} \rangle = \frac{1}{\sqrt{2\pi\sigma} \text{erf}(1/\sqrt{2}\sigma)} \int_{-\pi/2}^{\pi/2} \exp\left[-\left(\frac{\sin \delta}{\sqrt{2}\sigma}\right)^2\right] \cos^2 \delta d\delta. \quad (28)$$

This expression leads to the integral representation given in Section 3, Eq. (22).

Consider the experimental configuration adopted for the investigation of first-order interference (Fig. 4). The photon source was a mode-locked Nd:YAG laser (model Coherent-Antares), operating at a repetition rate of 76-MHz frequency, upconverted by third-harmonic generation (THG) and emitting 50-ps coherent light pulses with wavelength  $\lambda = 354.7$  nm. These pulses excited a collinear SPDC process in a 1-mm-thick  $\beta$ -barium borate NL crystal cut for type II collinear phase matching at an

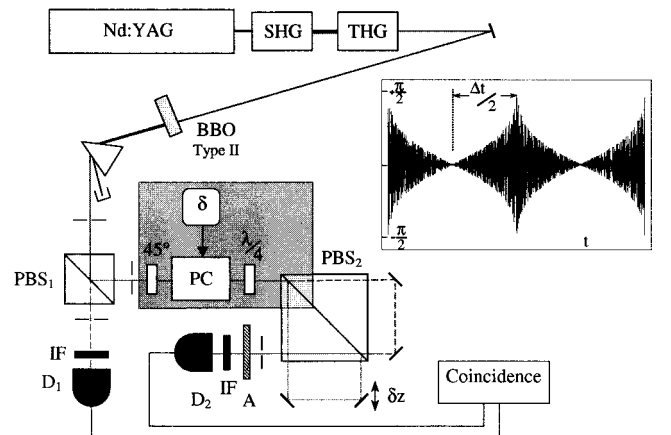


Fig. 4. Experimental apparatus for first-order stochastic interferometry.

angle  $49.4^\circ$  with respect to the optical axis. The two emitted correlated photons, polarized along the orthogonal  $\pi$  directions ( $o$ ,  $e$ ), corresponding to the optical axes of the crystal, were selected at the common wavelength  $\lambda = 709.4$  nm. One of the photons was transmitted through the polarizing beam splitter (PBS<sub>1</sub>) located in front of Sto-BS in Fig. 4 and detected by D<sub>1</sub>.

The corresponding output signal was adopted as the trigger for the conditional measurement performed by detector D<sub>2</sub> placed at the output of the Sto-IF apparatus. The radiation detected by D<sub>1</sub> and D<sub>2</sub> was filtered by two corresponding equal interference filters (IFs) with bandwidth  $\Delta\lambda = 6$  nm. The detectors were Si avalanche photon-counting modules EGG-SPCM200 with quantum efficiencies  $\approx 65\%$ . The output signals of the D's fed a coincidence counter within time windows of 5 ns.

The photon emerging from the Sto-BS device (expressed by the gray area in Fig. 4), followed suitable optical paths within the single polarizing beam splitter PBS<sub>2</sub> to realize, with two couples of external mirrors, the standard Mach-Zehnder interferometer (MZ-If) configuration.<sup>29</sup> The arms of the MZ-If were associated with the orthogonal states of the  $\pi$  polarization ( $o$ ,  $e$ ). In order to restore the indistinguishability between the optical paths of MZ-If, a  $\pi$  analyzer A, oriented at  $45^\circ$  with respect to ( $o$ ,  $e$ ), was inserted in front of D<sub>2</sub>. Fringe-visibility patterns were obtained and registered by varying the optical-path difference  $\delta z$  between the two arms of the MZ-If by a piezoelectric translation drive.

The main element of the Sto-BS was a transversely modulated LiNbO<sub>3</sub> Pockels cell, with a characteristic phase-shift voltage  $V_{\pi/2} = (282 \pm 8)V$  at  $\lambda = 709.4$  nm. The Pockels cell was driven by an adjustable generator that supplied the high-voltage waveform expressed by  $v(t) = A(t) u(ft)$  with  $u(ft)$  being a cw zero-mean square-wave carrier with a first-harmonic frequency  $f = 100$  kHz, amplitude modulated by a waveform  $A(t)$ .<sup>10,11</sup> The overall signal consisted of a periodic sequence of equal positive quasi-triangular pulses with duration  $\Delta t = 1.4$  ms, each starting at a different time  $t_j = (t_{j-1} + \Delta t)$  and expressed by  $A_j(t) = \sin^{-1}[g(\tau)]$  within  $0 \leq \tau \leq 1$ ,  $\tau \equiv 2(t - t_j)/\Delta\tau$ . Each triangular pulse of the sequence was completed in the interval  $1 \leq \tau \leq 2$  by a pulse equal to  $A_j(\tau)$  but symmetrical in time, i.e., having in common with  $A_j(t)$  the maximum voltage value and decreasing toward zero with negative slope. In these expressions the function  $g(\tau) \equiv |x(\tau)|$  is the solution of the equation  $2p(x|\sigma) = d\tau(|x|)/d|x|$ . The  $\sin^{-1}$  dependence of  $A_j(t)$  accounts for the Malus law of polarization, and  $g(\tau)$  expresses the effect of the distribution function  $p(x|\sigma)$  of the driving signal. The function  $A_j(\tau)$  was synthesized, for different values of  $\sigma$ , by electrically programmable read-only memory devices. The inset of Fig. 4 shows the electrical waveform  $v(t)$ , normalized to its maximum amplitude  $V_{\pi/2}$  and related to the Gaussian distribution  $p(x|\sigma)$  given in Eq. (1) with  $\sigma = 0.5$ . Alternatively, a truly stochastic excitation was provided by a carrier  $u(ft)$  supplied by a narrow-band Gaussian noise source having a Lorentzian spectrum with  $\delta f/f \approx 0.1$  and a center frequency  $f \approx 100$  kHz. Further details on the Pockels cell driving are found in Refs. 10 and 11.

The experiment was performed by collecting several statistical samples of the measured visibility corresponding to different values of  $\sigma$  (varying in the range 0.3–100) and by comparing in each case the visibility obtained in stochastic conditions ( $\sigma \neq 0$ ) with that measured in stationary conditions ( $\sigma = 0$ ). In this way, we could obtain directly the average reduction of visibility for different values of the noise parameter  $\sigma$ .

The experimental results of the average visibility  $V_m^{(1)}$  versus  $\sigma$  are shown in Fig. 3. The best fit gives a visibility reduction for increasing  $\sigma$  of  $\sim 20\%$ , in agreement with the theoretical predictions and with the experimental results previously obtained for coherent light (see Fig. 2 of Ref. 10). The best-fit curve representing the results is calculated by assuming that the stochasticity parameter  $x$  varies within the reduced interval  $[-0.9, 0.9]$  instead of the integration interval  $[-1, 1]$  appearing in the theoretical result expressed by Eq. (21). This reduction of domain of stochastic variation is due to a noncomplete randomization of the  $R$  and  $T$  optical parameters of the Sto-BS obtainable with our experimental EO driving system. Precisely, the EO response of the adopted Pockels cell could not follow the 100-kHz modulation frequency of the driving high-voltage electric noise generator. Another possible source of disturbance is the presence of acoustic-wave resonances in the LiNbO<sub>3</sub> crystal of our EO device caused by piezoelectric ringing for driving frequencies larger than 100 kHz.<sup>30</sup>

## 4. SECOND-ORDER STOCHASTIC INTERFEROMETRY

### A. Theory

The process of stochastic interferometry involving a two-photon state may be modeled by consideration of two entirely different optical schemes corresponding to experiments carried out so far in the stationary regime. A stochastic extension of these two different schemes is shown by the two drawings in Fig. 5.

Consider first the scheme shown in Fig. 5(a), where each incoming photon particle with equal  $\pi$  polarization excites one of the two input modes  $k_j$  ( $j = 1, 2$ ) of a symmetric beam splitter (BS), having the respective states previously stochastically phase shifted by  $(\pi/2 + \delta_1)$  and  $(\pi/2 + \delta_2)$  by two equal (quarter-wave plate plus Pockels cell) EO devices. This is the mixed-state injected version of the well known stationary secondary-order interferometer, first introduced by Mandel and coworkers<sup>15</sup> and by Alley and coworkers.<sup>16</sup>

The effect of the overall input device is represented by the unitary operator:

$$\begin{aligned} \hat{V}_h(S_h) &= \exp\left[i\left(\frac{\delta_h}{2} + \frac{\pi}{4}\right)\hat{\sigma}_x\right] \\ &= \cos\left(\frac{\delta_h}{2} + \frac{\pi}{4}\right)\hat{I} + i\sin\left(\frac{\delta_h}{2} + \frac{\pi}{4}\right)\hat{\sigma}_x, \end{aligned} \quad (29)$$

where  $S_h = R_x(\delta_h + \pi/2)$  and  $h = 1, 2$ . In the case of equal input ( $o$ ) polarization for the two photons the final state lies on the  $y, z$  plane of the Poincaré sphere; i.e., it is elliptically polarized.

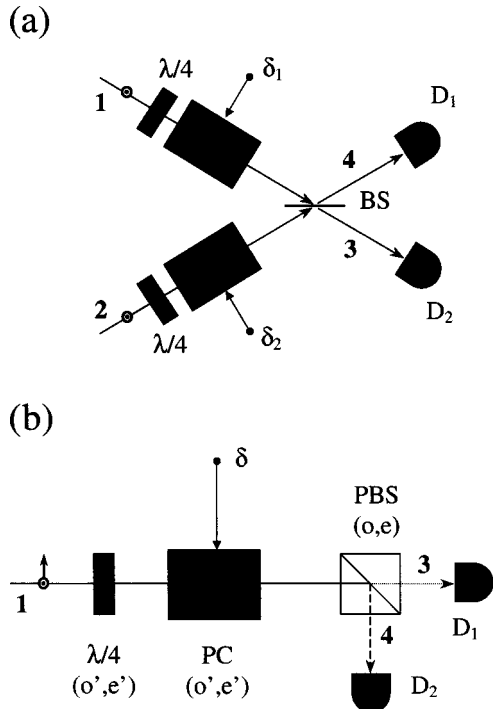


Fig. 5. Second-order Sto-BS: (a) noncollinear case, (b) collinear case.

Assume the input product state:

$$|\Psi\rangle_{\text{in}} = |\psi_1\rangle_1 \otimes |\psi_2\rangle_2, \quad (30)$$

where  $|\psi_j\rangle_\alpha$  is the  $|\psi_j\rangle$  polarization state for the  $\alpha$  mode. The state after transformation and before injection in the BS is

$$|\Psi\rangle_{\text{int}} = \hat{V}_1|\psi_1\rangle_1 \otimes \hat{V}_2|\psi_2\rangle_2. \quad (31)$$

The state after the linear superposition in the BS, characterized by parameters  $t$ ,  $r$ , and  $|t|^2 + |r|^2 = 1$ , is

$$|\Psi\rangle_{\text{out}} = [t|\tilde{\psi}_1\rangle_3 + r|\tilde{\psi}_1\rangle_4] \otimes [t|\tilde{\psi}_2\rangle_{4'} + r|\tilde{\psi}_2\rangle_{3'}], \quad (32)$$

with  $|\tilde{\psi}_j\rangle_\alpha = \hat{V}_j|\psi_j\rangle_\alpha$ . Prime and unprimed indexes account for the detector excitation at the different times,  $t$  and  $t + \tau$ . In order to refer more precisely to the experimental conditions, the time  $t$  accounts for the temporal position of the center of mass of the photon wave packet (wp) assumed Gaussian with a full width expressed by the photon's coherence time  $\tau_{\text{coh}}$ .

Expression (32) can be written as

$$|\Psi\rangle_{\text{out}} = [t^2|\tilde{\psi}_1\rangle_3 \otimes |\tilde{\psi}_2\rangle_{4'} + r^2|\tilde{\psi}_1\rangle_4 \otimes |\tilde{\psi}_2\rangle_{3'}] + \text{tr}[\tilde{\psi}_1\rangle_3 \otimes |\tilde{\psi}_2\rangle_{3'} + |\tilde{\psi}_1\rangle_4 \otimes |\tilde{\psi}_2\rangle_{4'}], \quad (33)$$

where the two square brackets account, respectively, for single-photon coincidences involving detection on both output modes and for two-photon detection on either one of the output modes.

The intensity correlation measurement, performed by two equal single-photon detectors  $D_j$  coupled to both output modes of a single BS, is evaluated by the average:

$$\text{out}\langle\Psi|\sum_{j,l}^{o,e} \sum_k^{3,3'} \sum_q^{4,4'} : \hat{E}_{jk}^{(-)} \hat{E}_{jk}^{(+)} \hat{E}_{lq}^{(-)} \hat{E}_{lq}^{(+)} : |\Psi\rangle_{\text{out}}. \quad (34)$$

This procedure postselects the first contribution of Eq. (33).

In case of overlap of the photon wps,  $\tau \ll \tau_{\text{coh}}$ , on the BS, the coincidence rate is found:

$$R_0 = \Gamma[|t|^4 + |r|^4 + t^2 r^{*2} |\langle\tilde{\psi}_2|\tilde{\psi}_1\rangle|^2 + \text{c.c.}], \quad (35)$$

where  $\Gamma$  is an appropriate proportionality factor. For no wp overlap the interference term disappears and

$$R_\infty = \Gamma[|t|^4 + |r|^4]. \quad (36)$$

The second-order interference visibility  $V^{(2)}$  is defined in the same way as for the first-order case. For wp overlap it is found

$$V^{(2)} = \frac{|R_\infty - R_0|}{R_\infty} = \frac{2|r|^2|t|^2}{|t|^4 + |r|^4} |\langle\tilde{\psi}_2|\tilde{\psi}_1\rangle|^2. \quad (37)$$

and, for no wp overlap,  $V^{(2)} = 0$ . In the case of a lossless symmetric beam splitter,<sup>31</sup>  $V^{(2)} = |\langle\tilde{\psi}_2|\tilde{\psi}_1\rangle|^2$ , which depends on the mutual projection of the two-photon polarization states transformed by the operator (29). For  $\delta_1 = \delta_2$ , i.e.,  $\hat{V}_1 = \hat{V}_2$ , i.e., for a fully in-phase  $\pi$  transformation, the visibility attains its maximum value:  $V^{(2)} = 1$ . In general, for an input product state  $|\Psi\rangle_{\text{in}} = |o\rangle_1 \otimes |o\rangle_2$ , it is found

$$V^{(2)}(\delta_1, \delta_2) = \frac{1}{2} [1 + \cos(\delta_1 - \delta_2)], \quad (38)$$

which shows the effect of the phase shift  $\delta_1 - \delta_2$  in the stochastic regime. For two statistically independent  $\delta_{1,2}$  Gaussian phase distributions, with the same  $\sigma$ , we obtain

$$\langle V^{(2)} \rangle(\sigma) = \frac{1}{2} \{ [1 + \langle V^{(1)} \rangle(\sigma)]^2 \}. \quad (39)$$

The dashed curve of Fig. 6 shows the behavior of

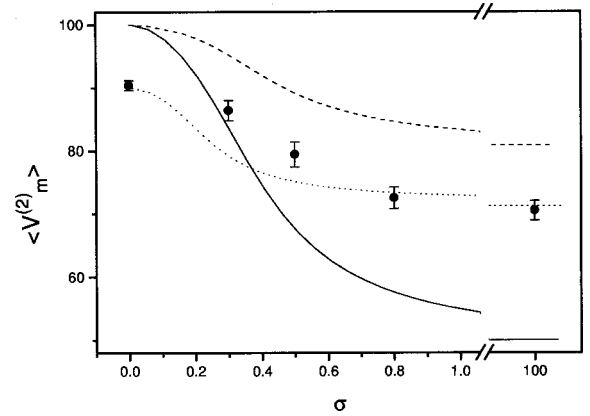


Fig. 6. Second-order fringe visibility  $\langle V^{(2)} \rangle$  as a function of the stochastic parameter  $\sigma$ . The dashed curve corresponds to the expression of the theoretical  $\langle V^{(2)} \rangle$  for the noncollinear case, Eq. (39). The solid curve represents the curve for  $\langle V^{(2)} \rangle$  in the collinear case, Eq. (57). It can be compared with the dotted curve, which corresponds to the best-fit representation of the experimental data.

$\langle V^{(2)}(\sigma) \rangle$  as a function of  $\sigma$ . In the limit of a uniform distribution,  $\sigma \rightarrow \infty$ , the second-order visibility is  $\langle V^{(2)} \rangle = \frac{1}{2}[1 + (\pi/4)^2] \cong 0.808$ .

Assume now an input  $\pi$ -polarization entangled state:

$$|\Psi\rangle_{\text{in}} = \frac{1}{\sqrt{2}}[|\psi_a\rangle_1 \otimes |\psi_b\rangle_2 + \exp(i\phi)|\psi_b\rangle_1 \otimes |\psi_a\rangle_2]. \quad (40)$$

The transformation in terms of the operator (29) is

$$|\psi\rangle_{\text{int}} = \frac{1}{\sqrt{2}}[|\tilde{\psi}_a^1\rangle_1 \otimes |\tilde{\psi}_b^2\rangle_2 + \exp(i\phi)|\tilde{\psi}_b^1\rangle_1 \otimes |\tilde{\psi}_a^2\rangle_2], \quad (41)$$

where  $|\tilde{\psi}_{a/j}^k\rangle = \hat{V}_k|\psi_a\rangle_j$ . After the BS superposition, we have

$$\begin{aligned} |\Psi\rangle_{\text{out}} = & \frac{1}{\sqrt{2}}[t^2|\tilde{\psi}_a^1\rangle_3 \otimes |\tilde{\psi}_b^2\rangle_{4'} + r^2|\tilde{\psi}_b^2\rangle_3 \otimes |\tilde{\psi}_a^1\rangle_{4'} \\ & + \exp(i\phi)(t^2|\tilde{\psi}_b^1\rangle_3 \otimes |\tilde{\psi}_a^2\rangle_{4'} + r^2|\tilde{\psi}_a^2\rangle_3 \otimes |\tilde{\psi}_b^1\rangle_{4'}) \\ & + |\text{NoCoinc} \rangle. \end{aligned} \quad (42)$$

The  $|\text{NoCoinc} \rangle$  state accounts for two-photon detection on one output mode and does not lead to coincidences.

The coincidence rate detected on both output modes is the average of expression (34) over the input state. In case of full photon wp's overlapping,  $\tau \ll \tau_{\text{coh}}$ , it is found,

$$\begin{aligned} R_0 = & \Gamma[|t|^4 + |r|^4][1 + |\langle\psi_a|\psi_b\rangle|^2 \cos \phi] \\ & + t^2 r^{*2} \Re[\langle\tilde{\psi}_b^2|\tilde{\psi}_b^1\rangle\langle\tilde{\psi}_a^1|\tilde{\psi}_a^2\rangle \exp(i\phi)] + \text{c.c.}], \end{aligned} \quad (43)$$

which reduces, in the absence of overlap, to

$$R_\infty = \Gamma[|t|^4 + |r|^4][1 + |\langle\psi_a|\psi_b\rangle|^2 \cos \phi]. \quad (44)$$

The second-order interference visibility is

$$V^{(2)} = \frac{2|r|^2|t|^2}{|t|^4 + |r|^4} |\Re[\langle\tilde{\psi}_b^2|\tilde{\psi}_b^1\rangle\langle\tilde{\psi}_a^1|\tilde{\psi}_a^2\rangle \exp(i\phi)]|, \quad (45)$$

which depends on the entanglement phase  $\phi$ . For the input state  $|\Psi\rangle_{\text{in}} = 1/\sqrt{2}[|o\rangle_1 \otimes |e\rangle_2 + \exp(i\phi)|e\rangle_1 \otimes |o\rangle_2]$  and a lossless symmetric BS we obtain the expression

$$V^{(2)}(\delta_1, \delta_2; \phi) = \frac{1}{2}[1 + \cos(\delta_1 - \delta_2)]|\cos(\phi)|, \quad (46)$$

which coincides with that obtained for the case of an input product state but with a new factor accounting for the entanglement phase.

If we consider the same experimental configuration shown by Fig. 5(a) with the normal BS replaced by a polarizing beam splitter, we have the stochastic counterpart of the second-order interferometer. In this case, we obtain the expression of the second-order visibility for the input product state,

$$V^{(2)}(\delta_1, \delta_2) = \frac{\cos \delta_1 \cos \delta_2}{1 + \sin \delta_1 \sin \delta_2}, \quad (47)$$

and for the input entangled state,

$$\begin{aligned} V^{(2)}(\delta_1, \delta_2; \phi) & = \frac{\cos \delta_1 \cos \delta_2 + (1 - \sin \delta_1 \sin \delta_2) \cos \phi}{1 - \sin \delta_1 \sin \delta_2 + \cos \delta_1 \cos \delta_2 \cos \phi}. \end{aligned} \quad (48)$$

Consider now the second-order Sto-IF shown by the configuration given in Fig. 5(b), which coincides with that adopted in our experiment. The two-photon state, expressed as  $|\Psi\rangle_{\text{in}} = |o\rangle \otimes |e\rangle$  and generated in a type II NL crystal by collinear SPDC, propagates through a quarter-wave plate ( $\lambda/4$ ) and a Pockels cell (PC) before being processed by a polarizing beam splitter (PBS). This second-order polarization-interference method, to our knowledge, has been first adopted in our laboratory.<sup>32</sup> Consider the effect of the transformation expressed by the Sto-BS operator (29) on the input  $\pi$ -polarization state of two photons generated with mutual delay  $\tau$ :  $|\Psi\rangle_{\text{in}} = |\psi_1\rangle_1 \otimes |\psi_2\rangle_{1'}$ . By adoption of the same notation as for the noncollinear case, we have

$$|\Psi\rangle_{\text{int}} = |\tilde{\psi}_1\rangle_1 \otimes |\tilde{\psi}_2\rangle_{1'}. \quad (49)$$

The state emerging from the PBS, which transmits and reflects the  $o$  and the  $e$  polarizations, respectively, is the output state and is written as

$$|\Psi\rangle_{\text{out}} = [c_{o1,e2}|o\rangle_3 \otimes |e\rangle_{4'} + c_{e1,o2}|e\rangle_4 \otimes |o\rangle_{3'}] \quad (50)$$

$$+ [c_{o1,o2}|o\rangle_3 \otimes |o\rangle_{3'} + c_{e1,e2}|e\rangle_4 \otimes |e\rangle_{4'}], \quad (51)$$

where  $c_{jk,lq} = \langle j|\tilde{\psi}_k\rangle\langle l|\tilde{\psi}_q\rangle$ , with  $j, l = o, e$  and  $k, q = 1, 2$ , corresponds to the product of the projections of the photon polarization state on the PBS basis. We expect interference when the two photons wp's overlap:  $\tau \ll \tau_{\text{coh}}$ . However, when this is not the case, the interference disappears, as we shall see, and the two particles are split by the PBS as classical particles.

The intensity correlation at the output of the PBS is expressed by the average of the operator (34) over the input state that postselects in this way the first contribution of Eq. (50).<sup>33,34</sup>

In the present interferometry experiment the measurements are carried out by both detectors  $D_j$ , and the measured quantity is the number of coincidence detections counted within a suitable time window. The coincidence rates for photon wp's overlap and nonoverlap are given respectively by

$$R_0 = \Gamma|\langle o|\tilde{\psi}_1\rangle\langle e|\tilde{\psi}_2\rangle + \langle e|\tilde{\psi}_1\rangle\langle o|\tilde{\psi}_2\rangle|^2, \quad (52)$$

$$R_\infty = \Gamma[|\langle o|\tilde{\psi}_1\rangle\langle e|\tilde{\psi}_2\rangle|^2 + |\langle e|\tilde{\psi}_1\rangle\langle o|\tilde{\psi}_2\rangle|^2]. \quad (53)$$

The second-order visibility (37) is then generally expressed by

$$V^{(2)} = 2 \frac{|\langle o|\tilde{\psi}_1\rangle\langle e|\tilde{\psi}_2\rangle\langle e|\tilde{\psi}_1\rangle\langle o|\tilde{\psi}_2\rangle|}{|\langle o|\tilde{\psi}_1\rangle\langle e|\tilde{\psi}_2\rangle|^2 + |\langle e|\tilde{\psi}_1\rangle\langle o|\tilde{\psi}_2\rangle|^2}. \quad (54)$$

For an input state  $|\Psi\rangle_{\text{in}} = |o\rangle_1 \otimes |e\rangle_{1'}$ , the above formula reduces to

$$V^{(2)}(\delta) = \frac{\cos^2 \delta}{1 + \sin^2 \delta}. \quad (55)$$

Note that Eq. (47) reduces to Eq. (55) for  $\delta_1 = \delta_2$ . This means that the collinear case is equivalent to the noncollinear case, operating with a polarizing beam splitter and with injection of a product state or of a singlet entangled state ( $\phi = \pi/2$ ).

As in the case of first-order interferometry, the average value of the visibility with respect to the stochasticity parameter  $x = \sin \delta$  is calculated by means of the expression

$$\langle V^{(2)}(x) \rangle_x = \int_{-1}^{+1} p(x) V^{(2)}(x) dx. \quad (56)$$

However, experimentally we can measure the mean values  $\langle R_0 \rangle_x$  and  $\langle R_\infty \rangle_x$ , and hence we can obtain the experimental mean visibility:

$$\langle V_m^{(2)}(\sigma) \rangle = |\langle R_\infty \rangle_x - \langle R_0 \rangle_x| / \langle R_0 \rangle_x. \quad (57)$$

The theoretical behavior of  $\langle V^{(2)}(\sigma) \rangle$  as a function of  $\sigma$  is reported in Fig. 6 (solid curve). In the limit  $\sigma \rightarrow \infty$  we have  $\langle V^{(2)} \rangle = 1/2$ .

## B. Experiment

A second-order stochastic interferometry experiment was performed by adopting the optical configuration shown in Fig. 5(b). A detailed experimental layout is given in Fig. 7. The correlated photons of each pair were SPDC generated at the same  $\lambda = 709.4$  nm with a coherence time  $\tau_{\text{coh}} = 100$  fs by a type II ( $\beta$ -barium borate) crystal cut for collinear emission with the same third-harmonic-generated mode-locked laser apparatus described in Section 3. In the condition of collinear emission, both emitted photons belong to the same spatial mode  $\mathbf{k}$  and have mutually orthogonal linear  $\pi$  polarizations, directed along the ordinary ( $o$ ) and extraordinary ( $e$ ) axes of the crystal.<sup>14</sup> Generally, at the exit of the NL crystal the two photon wp's do not overlap because of the crystal birefringence and the different group velocities. In the experiment this effect was fully compensated by two couples of micrometrically adjustable mirrors placed at the exit modes of a polarizing beam splitter PBS<sub>1</sub> shown in Fig. 7. The two-photon product state  $|\Psi\rangle = |oe\rangle \equiv |o\rangle \otimes |e\rangle$  was transmitted through the Sto-BS, corresponding to the sequence of optical elements located within the gray area of Fig. 7.

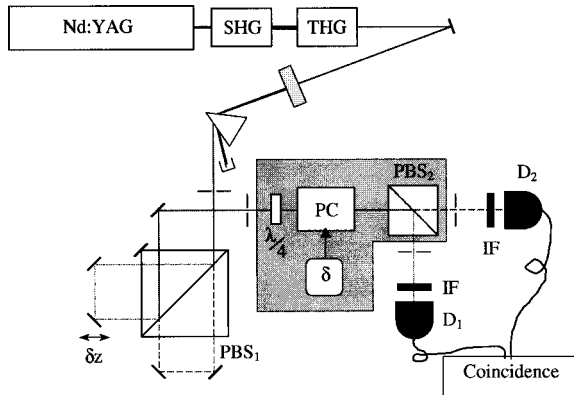


Fig. 7. Experimental apparatus for second-order stochastic interferometry.

The photons emerging from the two output sides of the polarizing beam splitter PBS<sub>2</sub> were detected by D<sub>1</sub> and D<sub>2</sub> after filtering by two equal IF's having a bandwidth  $\Delta\lambda = 6$  nm. The Sto-BS and the related  $\delta$ -driving devices were identical to the one described in Section 3.<sup>10,11</sup>

As in the case of the first-order interference measurements, the experiment was performed by collecting several statistical samples of the second-order visibility for different values of the variance of the stochastic parameter  $\sigma$ . Figure 6 shows the experimental results corresponding to the measurements of  $\langle V_m^{(2)} \rangle$  as a function of  $\sigma$ . Note there the loss of the visibility for increasing values of  $\sigma$  starting from the stationary condition value  $\sigma = 0$ . The experimental results and the corresponding best fit (see the dotted curve of Fig. 6) give a  $\sim 20\%$  variation of the second-order visibility, which is lower than the theoretical prediction of 50% given by the solid curve of the same Fig. 6. We believe that this effect can be attributed to the same limitations of the frequency response of the EO modulator, already discussed in connection with the results of the first-order Sto-IF experiment.<sup>30</sup> This problem is caused by the incomplete randomization of the beam-splitter parameters. As a consequence, the shape of the distribution of the stochasticity parameter  $\sigma$  and the amount of the visibility variation are modified.

## 5. CONCLUSION

In conclusion, we have reported, for the first time to our knowledge, a full theoretical account of the first- and second-order interferometry in the stochastic regime by a Fock-state photon excitation. The theoretical results were substantiated by two experiments involving the modern technique of nonlinear spontaneous parametric downconversion. We believe that the present results are relevant for a deeper understanding of the statistical properties of quantum particles within the fundamental framework of field interferometry operating in exotic conditions.

This study was supported by the Progetto di Ricerca Avanzata of the Istituto Nazionale per la Fisica della Materia (PRA-Cat 97), by the Ministero per l'Universita' e per la Ricerca Scientifica e Tecnologica, and by the Field-Effect-Transistor European Network IST-2000-29681 (Active Teleportation and Entangled States Information Technology) on Quantum Information.

## REFERENCES AND NOTES

1. W. K. Wootters and W. H. Zurek, "Complementarity in the double-slit experiment: quantum nonseparability and a quantitative statement of Bohr's principle," *Phys. Rev. D* **19**, 473–484 (1979).
2. L. S. Bartell, "Complementarity in the double-slit experiment: on simple realizable systems for observing intermediate particle-wave behavior," *Phys. Rev. D* **21**, 1698–1699 (1980).
3. M. Jammer, *The Philosophy of Quantum Mechanics* (Wiley, New York, 1974).
4. F. De Martini, "The concept of photon and the paradoxes of the complementarity in optics," in *Niels Bohr Symposium Proceedings, Roma, 1985*, *Riv. Storia Sci.* **2**, 557 (1985).
5. H. Rauch and J. Summhammer, "Static versus time-dependent absorption in neutron interferometry," *Phys. Lett. A* **104**, 44 (1984).

6. H. Rauch, J. Summhammer, and D. Tuppinger, "Stochastic and deterministic absorption in neutron-interference experiments," *Phys. Rev. A* **36**, 4447–4455 (1987).
7. F. De Martini and S. Di Fonzo, "Transition from Maxwell-Boltzmann to Bose-Einstein partition statistics by stochastic splitting of degenerate light," *Europhys. Lett.* **10**, 123–128 (1989).
8. F. De Martini, *Foundations of Quantum Mechanics*, M. O. Scully and M. M. Nieto, eds. (World Scientific, New York, 1992).
9. N. Hussain, N. Imoto, and R. Loudon, "Quantum theory of dynamic interference experiments," *Phys. Rev. A* **45**, 1987–1996 (1992).
10. F. De Martini, L. De Dominicis, V. Cioccolanti, and G. Milani, "Stochastic interferometer," *Phys. Rev. A* **45**, 5144–5151 (1992).
11. F. De Martini and L. De Dominicis, "Bose-Einstein photon correlations in the stochastic interferometer," *Opt. Lett.* **17**, 429–431 (1992).
12. J. A. Wheeler, "The past and the delayed-choice double slit experiment," *Mathematical Foundations of Quantum Theory*, A. R. Marlow, ed. (Academic, New York, 1978), pp. 250–253.
13. M. O. Scully, B. G. Englert, and J. Schwinger, "Spin coherence and Humpty-Dumpty. III. The effects of observation," *Phys. Rev. A* **40**, 1775–1784 (1989).
14. D. Klyshko, *Photons and Nonlinear Optics* (Gordon and Breach, New York, 1988).
15. Z. Y. Ou and L. Mandel, "Violation of Bell's inequality and classical probability in a two-photon correlation experiment," *Phys. Rev. Lett.* **61**, 50–53 (1988).
16. Y. Shih and C. Alley, "New type of Einstein-Podolsky-Rosen-Bohm experiment using pairs of light quanta produced by optical parametric down conversion," *Phys. Rev. Lett.* **61**, 2921–2924 (1988).
17. D. Boschi, F. De Martini, and G. Di Giuseppe, "Quantum interference and Feynman path indistinguishability for particles in entangled states," *Fortschr. Phys.* **46**, 6–14 (1998).
18. D. Bouwmeester, "The physics of quantum information: basic concepts," *The Physics of Quantum Information*, D. Bouwmeester, A. Ekert, and A. Zeilinger, eds. (Springer, Berlin, 2000), pp.1–14.
19. C. K. Hong and L. Mandel, "Experimental realization of a localized one-photon state," *Phys. Rev. Lett.* **56**, 58–60 (1986).
20. D. Stoler and B. Yurke, "Generating antibunched light from the output of a nondegenerate frequency converter," *Phys. Rev. A* **34**, 3143–3147 (1986).
21. B. Yurke and D. Stoler, "Measurement of amplitude probability distributions for photon-number-operator eigenstates," *Phys. Rev. A* **36**, 1955–1958 (1987).
22. B. E. A. Saleh and M. C. Teich, *Fundamentals of Photonics* (Wiley, New York, 1991), Chap. 6.
23. J. S. Gradshteyn and I. M. Ryzhik, *Tables of Integrals, Series, and Products* (Academic, San Diego, 1987).
24. F. De Martini, S. Di Fonzo, and R. Tommasini, in *Coherence and Quantum Optics VI*, J. Eberly, L. Mandel, and E. Wolf, eds. (Plenum, New York, 1990).
25. F. De Martini and R. Tommasini, "Transition from classical 'Maxwell-Boltzmann' to quantum Bose-Einstein partition statistics by stochastic scattering of degenerate light," in *New Frontiers of QED and Quantum Optics*, A. Barut, ed. (Plenum, New York, 1990), pp. 54–58.
26. B. De Finetti, *Theory of Probability* (Wiley, New York, 1975). The Fermi Dirac statistics has been obtained in the context of stochastic scattering by inserting in the integral of Eq. (11) a formal condition expressing a "particle exclusion principle," i.e., the occupancy 0 or 1 of the output modes: J. Tersoff and D. Bayer, "Quantum statistics for distinguishable particles," *Phys. Rev. Lett.* **50**, 553–554 (1983).
27. J. Sakurai, *Modern Quantum Mechanics* (Addison-Wesley, Reading, Mass., 1994).
28. J. Preskill, "Lecture notes for Physics 229: quantum information and computation," <http://www.theory.caltech.edu/~preskill/ph229>.
29. M. Born and E. Wolf, *Principles of Optics*, 6th ed. (Pergamon, Oxford, 1980).
30. X. D. Wang, P. Basseras, R. J. D. Miller, J. Sweetser, and I. A. Walmsley, "Regenerative pulse amplification in the 10-KHz range," *Opt. Lett.* **15**, 839–841 (1990).
31. L. De Caro and A. Garuccio, "Reliability of Bell-inequality measurements using polarization correlations in parametric-down-conversion photon sources," *Phys. Rev. A* **50**, R2803–R2805 (1994). In virtue of expressions (33) and (50) the factorizability of the product state is not affected by the unitary transformation performed by the Sto-BS. The effective entangled state is determined at the BS output by state postselection obtained by the coincidence photodetection process.
32. R. A. Campos, B. E. A. Saleh, and M. C. Teich, "Quantum-mechanical lossless beam splitter: SU(2) symmetry and photon statistics," *Phys. Rev. A* **40**, 13711384 (1989).
33. G. Di Giuseppe, Laurea thesis (Universita' di Roma "La Sapienza," Rome, 1995).
34. G. Di Giuseppe, L. Heiberger, F. De Martini, and A. V. Sergienko, "Quantum interference and indistinguishability with femtosecond pulses," *Phys. Rev. A* **56**, R21–R24 (1997).